Proceedings of the ASME 2015 International Design Engineering Technical Conferences and Computers and Information in Engineering Conference
IDETC/CIE 2015
August 2-5, 2015, Boston, Massachusetts, USA

DETC2015-46566

A METHOD FOR DESIGNING FLAT-FOLDABLE 3D POLYGONAL MODELS

Yuto Kase
University of Tsukuba
Ibaraki, Tsukuba, Japan

Yoshihiro Kanamori
University of Tsukuba
Ibaraki, Tsukuba, Japan

Jun Mitani
University of Tsukuba
Ibaraki, Tsukuba, Japan

ABSTRACT

We propose a method for designing targeted 3D polygonal models that can be folded flat, which consist of side panels as well as horizontal top and bottom panels. Vertically adjacent panels are connected by hinges at their horizontal edges. The models can be folded flat by pushing down the top panel, while they can be also deployed by pulling up the top panel. The key idea in making the model so that it can be folded flat is to add vertical slits along the edges of side panels; the horizontally adjacent side panels are separated in the folded state, and are connected to form a closed solid model in the deployed state. Our method takes the shapes of the top panel as well as the cross sections of the side panels as inputs. Users of our prototype system first simply draw the top panel as a convex polygon. They then draw polylines to specify the cross sections. Since the polyhedral model generated by the input data rarely satisfies flat-foldability conditions, our system modifies the positions of the vertices in cross sections based on numerical optimization. Unlike most origami design systems that ignore material thickness, our system can output the 3D geometry of panels so that they can be used to form a closed 3D model with a certain thickness.

1. INTORDUCTION

Folding objects compactly is essential to conserve storage space and carrying costs. Although objects made of thin soft materials are easy to fold, to make objects that consist of rigid materials foldable is not straightforward. We propose a method of designing polygonal models that can be folded flat that consist of rigid panels in this paper. We permit the edges to separate when the model is folded flat to simplify the problem, and we limit the shapes as follows. Our target models consist of rigid side panels as well as horizontal top and bottom panels, as shown in Figure 1. The side panels are connected vertically by hinges at their horizontal edges. We call the groups of side panels connected by hinges *side-panel chains* hereafter. For example, the model in Figure 1 has three side-panel chains. By pushing the top panel down, the model can be folded flat, while the model can be also deployed by pulling up the top panel. The key point is that all edges that are not connected by the hinges are separated in the folded state while the edges are connected to form a closed solid model in the deployed state.

Our method uses the shapes of the top panel as well as the cross-sections of the side-panel chains as inputs. Users simply first draw the top panel as a convex polygon in our prototype system. They then draw polylines to specify the cross sections. Since the polyhedral model generated by the input data rarely satisfies the flat-foldability conditions, our system modifies the positions of the vertices in cross sections based on numerical optimization. Each side panel is generated by perpendicularly sweeping the cross sections, and we can thus simplify the flat-foldability problem from that of 2D panels in 3D space into that of 1D line segments in 2D space. Our system then outputs the geometry of a flat-foldable polygonal model. Unlike most origami design systems that ignore material thickness, our system can output the 3D geometry of panels so that they can form a closed 3D model with a certain thickness.

Related studies are discussed in Section 2 of this paper and our method is described in Section 3. The results obtained with our new approach are presented in Section 4. Finally, our conclusions are presented in Section 5.

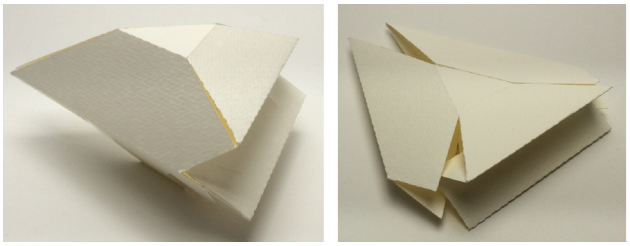

Figure 1. Example of flat-foldable polygonal models, which has a top and a bottom polygonal panels and three side-panel chains. The left photograph shows the deployed state while the right one the folded state.

2. RELATED WORK

Foldable structures have been widely studied in the area of origami engineering. Automobile airbags and solar panels on satellites are practical examples where objects must be compactly folded and instantly deployed when necessary. Origami engineering has contributed to improving the storability and portability of these products.

'Rigid origami' has been seriously discussed due to its importance in engineering in studies on foldable structures [1][2][3]. Rigid origami represents objects that consist of rigid panels joined by hinges and deform smoothly without any gaps. Designing rigid origami is a difficult problem because of its severe constraints.

Tachi proposed a method of designing rigid origami that can be folded flat [4]. However, the shapes designed with his method is limited to folding based on repeats of simple patterns. It is particularly difficult to design rigid origami as intended shapes. For example, it has been proven that no closed polyhedral model can be folded flat without holes by Cauchy [5]. Our approach avoids this difficulty by permitting the edges to separate in the folded state. Users can interactively design a model with a simple interface with some degree of flexibility under a limited shape domain.

There has been some software for origami design [6][7][8], and most of this has assumed that the material thickness is zero. Although a paper sheet is sufficiently thin to ignore thickness, we have to be aware of how thick material is in the design process. Handling the thickness of material is not a simple problem especially where more than three folding edges intersect at the same point. We have to consider the folding mechanism at the edges to avoid interference between panels. Tachi also propose a method that enable thick panels to be folded without deforming them by permitting holes to appear at the corners where folding edges meet [9]. The system we designed does not have any inner points where folding lines meet. We propose simple approaches that use hinges at the folding edges.

3. PROPOSED METHOD

Our target polygonal model consists of the top and the bottom panels as well as side-panel chains shown in Figure 1. The model in Figure 2 has a triangular top panel, and three side-panel chains. The whole shape is defined just by the shape of the top panel (red triangle in Figure 2) and the polylines (blue lines in Figure 2), which represent the cross-sections of the side-panel chains. Note that the shape of the bottom panel is also determined accordingly. Although our method first ignores material thickness, it can optionally take into consideration the thickness of panels. When the panels are thick, the system calculates the shape of each panel in 3D, and a way of applying two types of hinges.

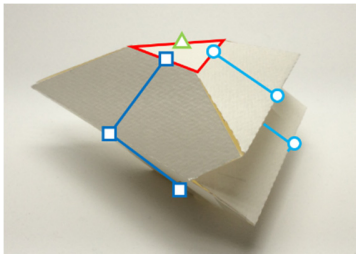

Figure 2. Example of polyhedral model that our method is target at. User inputs shapes of top and bottom panels and cross sections of side panels.

This section describes the method of designing a flat-foldable 3D polyhedral model. Our method involves six steps.

(1) Construct the initial polygonal model from user input.
(2) Find the best configuration for the folded state from all possible cases.
(3) Adjust the position of vertices in the cross-section of side-panel chains to satisfy flat-foldability conditions.
(4) Simulate the motion of the model during folding and deploying operations, and present the three dimensional computer graphics (3DCG) animation.
(5) Optionally add thickness to the panels.
(6) Modify the shape of the panels to avoid interference based on the types of hinges and their thickness.

The details on these steps are described in the following subsections.

3.1. Construction of Initial Polyhedral Model from User Input

The user first inputs the top panel as a polygon with N (>2) edges on a horizontal plane as well as its height, i.e., the distance from the bottom panel. The number of edges can be set arbitrarily. Figure 3 has an example of the input for the top panel with three vertices. $V_i \quad (i = 0, \cdots, N-1)$ represents a vertex of the top panel. Because the side panels are flattened and spread as seen in Figure 1, the top panel is limited to be convex to prevent adjacent side-panel chains from interfering with one another.

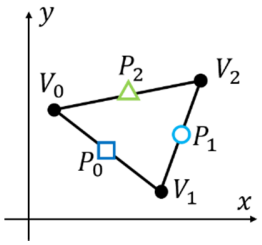

Figure 3. Convex shape of top panel. Midpoint P_i of each edge is initial point of polyline that forms each side-panel chain.

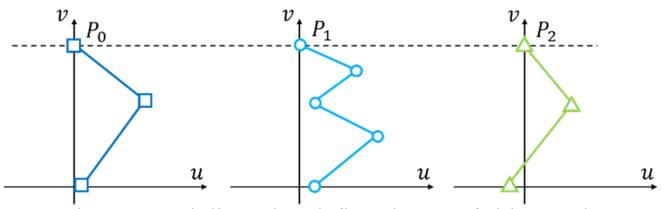

Figure 4. Polylines that define shapes of side panels.

The user next inputs the cross sections of the side-panel chains. The number of side-panel chains is defined by the number of edges of the top panel, i.e., number *N*. The user inputs each cross section as a polyline on the vertical plane that is perpendicular to each edge of the top panel. We have defined the uv-coordinate system on the plane as shown in Figure 4. Midpoint P_i of each edge of the top panel is initial point of polyline that forms each side-panel chain. The number of line segments on the polyline is arbitrary. Since the top and bottom panels are horizontal, the endpoints of each polyline share the same *v* coordinate. After the user has drawn the necessary polylines, each side panel is generated by calculating an infinite plane spanned by each line segment of a polyline and a horizontal edge and by trimming the infinite plane with other adjacent planes (Figure 5). The shape of the bottom panel is uniquely determined in this process.

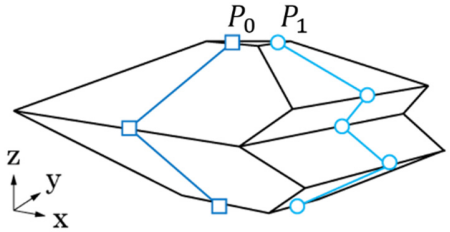

Figure 5. Polygonal model is generated from shape of top panel and polylines of cross sections.

3.2. Assignment of Direction of Folds at Each Hinge

The folding problem with side panels (a set of plane polygons that is in 3-dimensions) results in the problem with cross sections (a 1-dimensional polyline that is in 2-dimesions). The explanation in this section is independently applied to individual cross sections without dealing with others except for interference between nearby side panels. Let us consider a cross section that has M vertices on a uv plane in the following. Q_0 and Q_{M-1} correspond to the end points on the top and bottom panels. E_i is the edge between Q_i and Q_{i+1} $(i = 0, \cdots, M-2)$, whose length is l_i. Hinges, which can take any dihedral angle between 0 to 360º, are placed at each Q_i. When the cross section is flat-folded, each edge E_i is horizontally arranged while maintaining the continuity of the jointed edge. The geometric restrictions that each cross section has to satisfy are represented as Eqs. (1) and (2).

$$u'_i \geq u_i \text{ and} \quad (1)$$

$$gap = (u_{M-1} - u_0) - \sum_i \delta_i l_i = 0 \qquad (\delta_i \in \{-1,1\}) \quad (2)$$

u_i and u'_i in Eq. (1) correspond to the u-coordinate of Q_i before and after flat-folding. The condition represented by Eq. (1) prevents nearby side panels from interfering. If Eq. (1) is not satisfied, it means that the vertex moves inward of the solid when it is folded. As a result, the side panels in neighboring side-panel chains interfere in the folding process as can be seen in Figure 6.

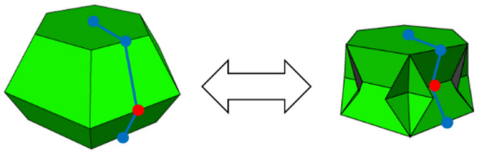
Figure 6. Shape in deployed state on the left shows that nearby panels penetrate each other in folded state on the right if the vertex (red) moves inward.

δ_i in Eq. (2) becomes 1 if E_i faces upward and -1 if downward (Figure 7). Because we have assumed that the top panel moves downward vertically a straight line, i.e., the u-coordinate is constant, the distance between the two end points of the side-panel chain in the u-coordinate have to be consistent both in flat-folded and deployed states. Eq. (2) represents this condition.
The angles of hinges become 0, 180, or 360º in the flat-folded state. Each angle corresponds to a mountain fold, flat state, and valley fold. As a result, every panel faces either upward or downward. If we ignore any geometrical restrictions, the total number of possible folded configurations is 2^{M-1} as outlined in Figure 7. However, even though all possible folded configurations are checked, Eq. (2) is not usually satisfied because the value of the *gap* takes discrete values based on the lengths of edges in the cross section that a user has freely drawn. Therefore, we first select the best configuration from those that satisfy Eq. (1), i.e., the best valley/flat/mountain assignment for hinges in the flat-folded state. Then, the system adjusts the position of the vertices of input polylines to enable them to satisfy Eq. (2) by employing numerical optimization.

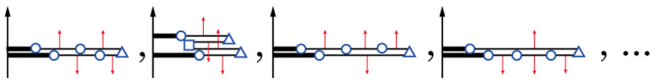
Figure 7. Example of folding configurations of cross section that has four panels and five hinges. Two bold lines represent top and bottom panels. Thin arrows represent normal directions of each edge. Symbols represent folding angles at hinges in folded state. Circles, triangles, and squares correspond to 180, 0, and 360º angles. There are $2^4 = 16$ configurations.

Because many of the configurations possibly satisfy Eq. (1), we selected the best one of them using certain criteria. We would like to make the model so that it could be folded smoothly. We assume that it would not be beneficial if a hinge had to be folded in the opposite direction. For example, it would be difficult to fold a hinge, whose angle was less than 180º (mountain fold) in a deployed state, into 360º (valley fold) in the flat-folded state.

We would like to make the change in the normal directions of each panel small for the same reason. We use the following formula to select the best configuration with these criteria as an objective function:

$$C_{total} = \omega_1 C_1 + \omega_2 C_2 + \omega_3 C_3 \quad (3)$$
$$C_1 = -\sum_i (n_i \times n_{i+1}) \cdot (0\ 0\ \rho_i)^{\mathrm{T}}$$
$$C_2 = -\sum_i n_i \cdot n'_i$$
$$C_3 = \frac{|gap|}{\sum_i l_i} M \quad .$$

Here, ρ_i takes 1, 0, or -1 based on the direction of the hinge at Q_i in the folded state. Each value corresponds to a mountain fold, flat state, and valley fold. n_i corresponds to unit normal vector of E_i in deployed state. With this setup, C_1 takes a small value when the assignments of folds for hinges are similar before and after being folded. n'_i corresponds to unit normal vector of E_i in folded states. Since the inner products of n_i and n'_i represent the cosine of the angle between normal vectors when the angle is small, i.e., the difference in the normal vectors is small, C_2 takes a smaller value. The gap is the left-hand-side value in Eq. (2). The system modifies the input cross section to satisfy Eq. (2) in the subsequent step. The amount of modification will be small if the gap is close to zero. Therefore C_3 is defined to minimize the gap. The total evaluation value, C_{total}, is defined as the weighted sum of C_1, C_2, and C_3.

The system selects the best configuration that minimize C_{total} from all possible mountain/valley assignments to hinges for each cross section. We simply set 1.0 for all w_1, w_2, and w_3. The positions of vertices Q_i in the cross section were then adjusted to make the value of the *gap* zero. We will describe how we adjusted them in the next subsection.

3.3. Modification of Cross Section

The positions of vertices Q_i in the cross section were adjusted to eliminate the *gap*, i.e., to satisfy Eq. (2) after we had selected the best configuration. To achieve this, we first update the edge length, l_i, at the rate of the length relative to the total length of edges. This means that l_i is updated as $l_i + \frac{l_i}{\sum_i l_i} gap$. With this update, the *gap* represented in Eq. (2) become zero. We then minimize the energy function, *E*, in Eq. (4) by using the steepest descent method so that the optimized cross section becomes approximately flat-foldable while keeping the modification small.

$$\begin{aligned} \mathrm{E} &= \omega_P \sum_i \left\| \hat{Q}_i - Q_i \right\|^2 + \omega_l \sum_i \left\| \hat{l}_i - l_i \right\|^2 \\ &= \omega_P \sum_i \{(\hat{u}_i - u_i)^2 + (\hat{v}_i - v_i)^2\} \\ &\quad + \omega_l \sum_i \left\{ \sqrt{(\hat{u}_i - \hat{u}_{i+1})^2 + (\hat{v}_i - \hat{v}_{i+1})^2} \right. \\ &\quad \left. - l_i \right\}^2 \qquad (4) \end{aligned}$$

where $\hat{Q}_i$ and $\hat{l}_i$ correspond to the adjusted vertex position and edge length. The first term in Eq. (4) makes the change in the input shape of the cross section small. The second term in Eq. (4) adjusts the length of the line segments to satisfy Eq. (2). ω_P and ω_l are their weights. Because the condition represented by Eq. (2) is more essential for flat-foldability, we set $\omega_P = 0.001$ and ω_l =1.0 based on our experiments. The system stops the optimization process when the gap becomes smaller than 0.001 of the average length of edges E_i, whose details are described in Section 5.

3.4. Folding Simulation

Previewing the folding motion in 3DCG is important to confirm the results before making a physical product. Because no side-panel chains interfere with other chains as long as Eq. (1) is satisfied, motion can be calculated independently for each side-panel chain. Since the bottom end point is fixed, and the top end point moves downward vertically a straight line, using inverse kinematics (IK) would be a solution to generating the motion of folding. However, it cannot be guaranteed that the side panels can be folded into a flat state, by simply specifying the positions of the two end points. In our method, we combine both forward kinematics (FK) and IK.

First, the system calculates the angle of each hinge at time *t* as follows.

$$(1-t)a_{initial} + ta_{folded} \quad (0 \le t \le 1) \quad (5)$$

where $a_{initial}$ is the initial angle and a_{folded} is the angle in the folded state of the hinge.

The shapes of the side-panel chains are calculated based on the angles by fixing the end point on the bottom panel. Then the system employs IK to adjust the position of the end point on the top panel. Furthermore, the system adjusts the height in the IK calculations to keep the height of all side-panel chains in the same level as shown in Figure 8.

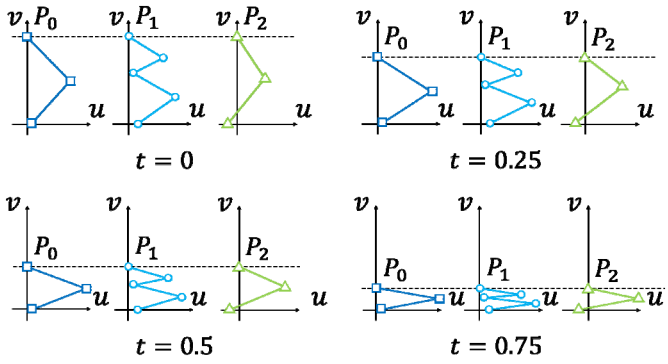

Figure 8. Shapes of side-panel chains in folding process. Heights of all chains are maintained the same.

3.5. Material Thickness

Although the thickness of material is ignored in most origami design systems, we have to take thickness into account when we create objects with thick material.

When we consider adding thickness to a zero-thickness polygon, there are three possibilities regarding which side to add thickness, i.e., adding thickness inward, outward, or both. If we use thick polygonal panels, we have to take interference into consideration. Further, we also have to consider the mechanism for hinges.

Here, we describe two different ways of adding thickness. The first is to add thickness to the outside of the polygonal model so that the inside space retains its designed shape. This is achieved by using hinges that have one rotational axis. The second way is to add half the material thickness to both sides of the polygonal model with two axis hinges.

3.5.1. Hinge Model with One Axis

A solid can close tightly as illustrated in Figure 9 by adding tapers to the edges of the panels.

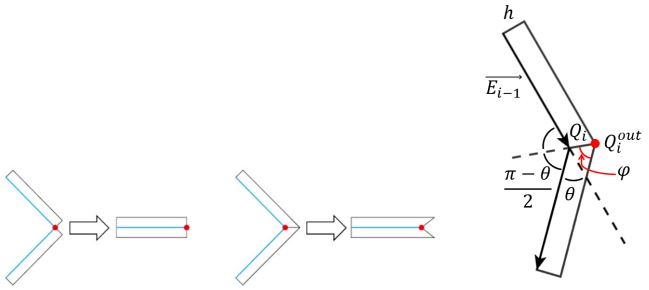

Figure 9. Panels on left are simple rectangular solids. Panels on middle are tapered at edges. Red dots represents locations of hinges. The taper angle is denoted as φ on right.

The angle of the tapers of the edges and the positions of hinges differ according to the direction of folding before and after being folded. Since there are mountain and valley cases in the initial state while mountain, valley, and flat cases in the folded state, there are six combinations for the direction of folding. The taper angle φ, and the location of the hinge for each case are summarized in Table 1. When hinges are positioned outside (denoted as 'out' in Table 1), its position Q_i^{out} is calculated as

$$Q_i^{out} = Q_i + \frac{h}{sin(\varphi)} R(\varphi) \frac{\overrightarrow{E_{i-1}}}{|\overrightarrow{E_{i-1}}|},$$

where $R(\cdot)$ is the rotation matrix and h is thickness.

Table 1. Relation between combinations of folding directions, taper angle φ and locations of hinges.

	Folding direction		φ	Location of Hinge
	Initial state	Folded state		
(a)	Mountain	Mountain	$(\pi-\theta)/2$	in
(b)		Valley	$(\pi-\theta)/2$	out
(c)		Flat	$\pi/2$	in
(d)	Valley	Mountain	$(\pi-\theta)/2+\theta$	in
(e)		Valley	$(\pi-\theta)/2+\theta$	out
(f)		Flat	$(\pi-\theta)/2+\theta$	in

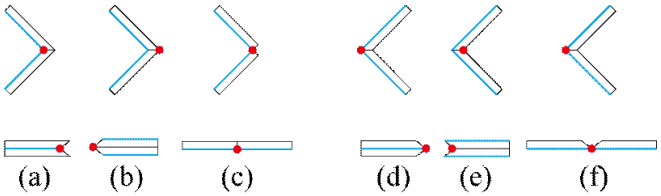

Figure 10. Cross section of side-panel chain, which has two panels connected by hinge. Six figures from left to right correspond to configurations listed in Table 1 from top to bottom. Bold lines are user-specified polylines. Red circles represent locations of hinges.

Figure 10 outlines the cross section of a side-panel chain, which has two panels connected by a hinge. The mechanism for the hinge is achieved simply by taping panels together at their edges. However, there are drawbacks in this structure; it is not strong sufficiently since the panels are connected at the ridge lines. Alternatively, we use hinges that have two rotating axes by adding thickness to both sides of the polygonal model, as described. There exist these hinges called *rolling contact joints*[10]. These hinges use flexible bands that create the necessary constraints to enforce a rolling movement between two panels. On the other hand our hinges use a panel bridging between two panels instead of flexible bands

3.5.2. Hinge Model with Two Axes

Hinges that have the two rotation axes in Figures 11 and 12 are commonly used to connect thick panels that are folded flat. The hinges can take arbitrary angles from 0 to 360º. These kinds of hinges are called *double hinges*. We have to modify the shape of the panel if we use these types of hinges as follows. First, we add a thickness of $h/2$ to both the inside and outside of the cross section for panel thickness h. We then modify the shapes of the edges of each panel to a semi-cylindrical shape so that they touch each other as in Figure 11. Further, we have to modify the shapes of the side edges of panels to avoid interference with nearby panels. The details on these modifications are described in the next subsection.

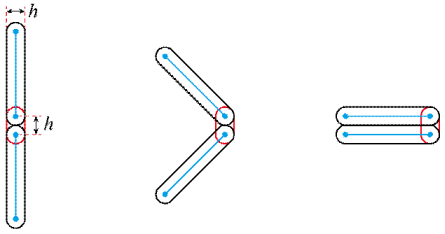

Figure 11. Illustrations of how to add thickness with double hinges.

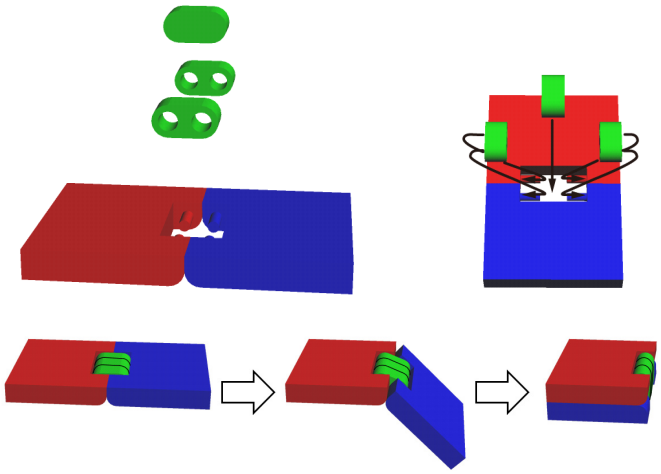

Figure 12. Assembly of the double hinge. Two thick panels connected by the double hinge can make arbitral angles.

3.5.3. Interferences Between Side Panels

Although 3D polyhedral models generated by the system described in Subsections 3.5.1 and 3.5.2 do not have interferences, if we add thickness to the panels, we have to consider interference between nearby side-panel chains. If position of a corner of a thick side panel does not satisfy Eq.(1), i.e. moves inward of the solid when it is folded, it interferes nearby panels as corner A in left of Figure 13. In such a case, the system removes the interfering volume by trimming the corner of the panel by the triangle A'BC as shown in right of Figure 13 to avoid the interference. A' is the point where A was moved in the direction perpendicular to the cross section of the side-panel chain so that the point satisfies Eq.(1). B is the point where edges of nearby side-panel chain crosses in folded state. And C is the vertex of the initial polygonal model.

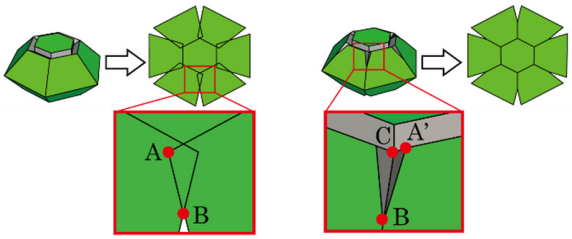

Figure 13. There exist interferences between nearby panels if we add thickness to the initial polygonal model (left). Corners are trimmed to avoid interferes (right).

4. RESULTS

We implemented the proposed method as a graphical user interface (GUI) application, and created prototype models. Here, we describe the results.

4.1. Adjustment of Input Cross Section

We designed a simple model that have three side-panel chains from input. Figure 14 shows the effect of the adjustment of vertex positions in the cross sections. The red polyline indicates the initial shape user-specified, and the blue polyline indicates the adjusted shape to satisfy the conditions in Eqs. (1) and (2). After the best configuration, i.e., mountain/flat/valley assignments were found, the position was calculated with the method described in Subsection 3.3. The maximum value of the distance between the initial and modified positions was 12.3 mm, and the average was 5.68 mm when we set the height to 12.9 cm. The maximum gap was 0.0335 mm when numerical optimizations converged.

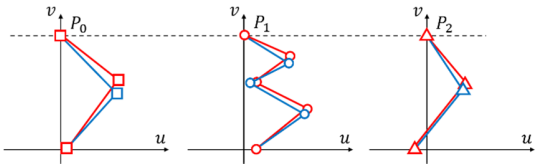

Figure 14. Red polyline indicates user input, and blue polyline indicates adjusted one.

4.2. Flat-foldable Polygonal Model without Thickness

The prototype models were made with paper sheets by converting designed 3D model data without thickness to 2D development. Figure 15 shows the 3D polygonal model and its development. The pairs of letters on edges represent the direction of folding before and after being folded. M, F, and V represent mountain folds, flat states, and valley folds, respectively. For example, (M, F) means the edge is a mountain before folding, and the edge becomes flat when the model is in a flat state. The assembled model is in Figure 1. The model is 10.5 cm in depth, 14.7 cm in width, and 8.0 cm in height when it is deployed.

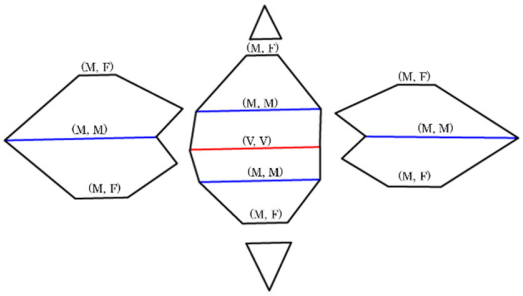

Figure 15. Development of the 3D polygonal model in Figure 1.

We similarly created a sphinx model as a more elaborate example, as shown in Figure 16. The model was 5.5 cm in depth, 17.2 cm in width and 8.7 cm in height. The calculation time for all processes was less than 1 second.

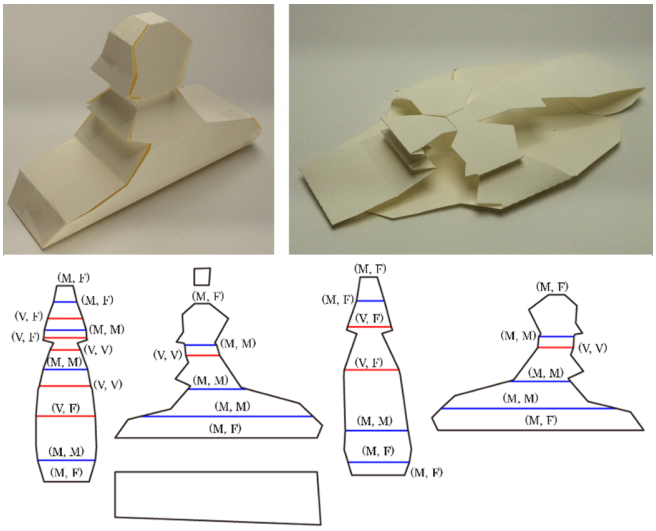

Figure 16. Sphinx model in deployed state (top left) and folded state (top right), and its development (bottom).

4.3. Flat-foldable Polygonal Model with Thickness

After we had designed a polygonal model, we added material thickness and hinge structures as described in Subsection 3.5. We made both the hinge models.

Figure 17 shows the prototype model whose hinges have one rotation axis. The prototype model in the upper row was 10.5 cm deep, 10.5 cm wide, 12.0 cm high, and 0.5 cm thick. When it is folded, it had four layers and is 10.0 cm in radius. After the system had generated 3D geometry data for the panels, the panels were printed out with a 3D printer. The hinges connected two panels were substituted by taping inside of the model.

Figure 18 shows the prototype model whose hinges had two rotation axes. The prototype in upper row was 4.0 cm deep, 3.5cm wide, 8.5cm high, and 0.5 cm thick. When it was folded, it had two layers and is 10.0 cm in radius.

The lower rows both in Figures 17 and 18 show CG images of the model in Figure 1 with thickness.

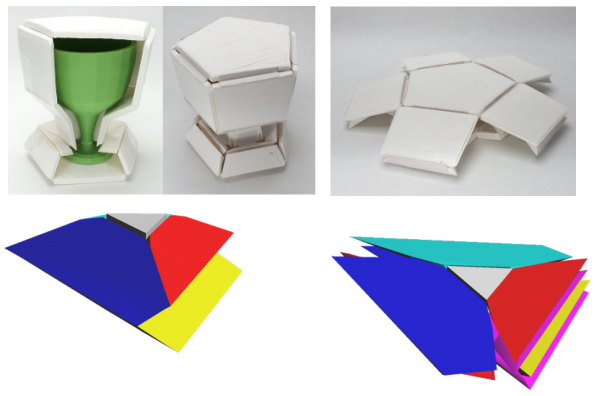

Figure 17. Prototypes of hinge model with one axis. Shapes in deployed state (left, center) and folded state (right). The photographs in the upper row are physical models, and the photographs in the lower row are CGs.

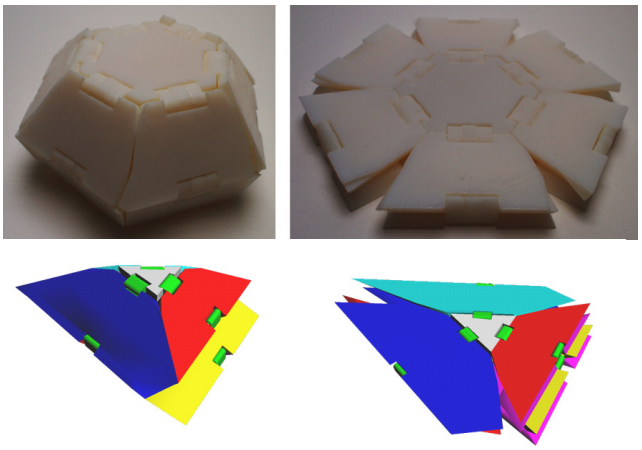

Figure 18. Prototype of hinge model with two axes. Shapes in deployed state (left) and folded state (right). The photographs in the upper row are physical models, and the photographs in the lower row are CGs.

5. CONCLUSION AND FUTURE WORK

We have proposed a method for designing flat-foldable polygonal models. We confirmed that flat foldable polygons can be designed with a simple user interface regardless of the thickness of materials using our method.

In future work, we intend to extend our method to handle polygonal models whose top panels are concave. Further, we intend to consider creating a more complex model by dividing the model into sub-parts. Although our method limits the trajectory of the top panel along a vertical straight line, if we allow other trajectories, more various shapes could be flat-folded. In addition, we need to consider mechanisms to keep the model stable in the deployed state.

REFERENCES

[1] Yves Klett, “REALTIME RIGID FOLDING ALGORITHM FOR QUADRILATERAL-BASED 1-DOF”, In Proceedings of the ASME 2013 International Design Engineering Technical Conferences & Computers and Information in Engineering Conference, 2013.

[2] Sicong LIU, Yan CHEN, and Guoxing LU, “THE RIGID ORIGAMI PATTERNS FOR FLAT SURFACE”, In Proceedings of the ASME 2013 International Design Engineering Technical Conferences & Computers and Information in Engineering Conference, 2013.

[3] Devin J. Balkcom, Erik D. Demaine, and Martin L. Demaine, “Folding Paper Shopping Bags”, in Abstracts from the 14th Annual Fall Workshop on Computational Geometry, Cambridge, Massachusetts, Nov. 19–20, 2004, pp. 14–15.

[4] Tomohiro Tachi, “Geoemtric Considerations for the Design of Rigid Origami Structures”, in Proceedings of IASS Symposium 2010, Shanghai, China, 2010, pp. 771-782.

[5] Cauchy, A. L., “Sur les polygons et le polyheders”, XVle Cahier IX, 1813, pp. 87-89.
[6] Jun Mitani, “ORI-REVO:A Design Tool for 3D Origami of Revolution”, http://mitani.cs.tsukuba.ac.jp/ori_revo/, (Jan. 25, 2015)
[7] Tomohiro Tachi, “Origamizer”, http://www.tsg.ne.jp/TT/software/index.html#origamizer, (Jan. 25, 2015)
[8] Robert J. Lang, “TreeMaker”, http://www.langorigami.com/science/computational/treemaker/treemaker.php, (Jan. 25, 2015)
[9] Tomohiro Tachi, “Rigid-foldable thick origami”, Origami5, 2011, pp. 253–263.
[10] Amélie Jeanneau, Just Herder, Thierry Laliberté and Clément Gosselin, “COMPLIANT ROLLING CONTACT JOINT AND ITS APPLICATION IN A 3-DOF PLANAR PARALLEL MECHANISM WITH KINEMATIC ANALYSIS”, In Proceedings of DETC’04 ASME 2004 Design Engineering Technical Conferences and Computers and Information in Engineering Conference, 2004, pp. 14-15.